Probabilistic Energy and Reserve Co-dispatch for High-renewable Power Systems and Its Convex Reformulation

Shuwei Xu, Wenchuan Wu, *Fellow*, *IEEE*, Bin Wang, and Yue Yang, *Member*, *IEEE*

***Abstract*—This paper proposes a probabilistic energy and reserve co-dispatch (PERD) model to address the strong uncertainties in high-renewable power systems. The expected costs of potential renewable energy curtailment/load shedding are fully considered in this model, which avoids insufficient or excessive emergency control capacity to produce more economical reserve decisions than conventional chance-constrained dispatch methods. Furthermore, an analytical reformulation approach of PERD is proposed to make it tractable. We firstly develop an approximation technique with high precision to convert the integral terms in objective functions into analytical ones. Then, the calculation of probabilistic constraints is equivalently transformed into an unconstrained optimization problem by introducing value-at-risk (VaR) representation. Specifically, the VaR formulas can be computed by a computationally-cheap dichotomy search algorithm. Finally, the PERD model is transformed into a convex problem, which can be solved reliably and efficiently using off-the-shelf solvers. Case studies are performed on IEEE test systems and real provincial power grids in China to illustrate the scalability and efficiency of the proposed method.**

***Index Terms*—Renewable energy, energy and reserve dispatch, emergency control, stochastic optimization, analytical approximation.**

NOMENCLATURE

A. Parameters and Constants

β	Pre-defined risk level
$1-\beta$	Confidence level in value of risk (VaR) formulas
ΔT	Length of each time period
γ_i	Power participation factor of unit i
$\omega_{t,m}$	Weight of component m
$\boldsymbol{\omega}, \boldsymbol{\mu}, \boldsymbol{\Sigma}$	Weight vector, expectation vector, and covariance matrix of Gaussian mixture model (GMM)
a_i, b_i, c_i	Cost coefficients of unit i
C_{CUR}	Cost coefficient of renewable energy curtailment ($/MW)
C_{LD}	Cost coefficient of load shedding ($/MW)
C_{UP}, C_{DN}	Cost coefficients of upward and downward reserve adjustments ($/MW)
D	Number of loads
$F_{C,t}, \hat{F}_{C,t}$	Integral cost and the corresponding approximated value in time period t
$G_{l,i}, G_{l,j}, G_{l,d}$	Power transfer distribution factors of line l
J	Number of renewable energy generations (REGs)
L	Number of transmission lines
$\bar{L}_l, \underline{L}_l$	Upper and lower flow limits of line l (MW)
M	Number of Gaussian components
N	Number of thermal units
$p_{d,t}$	Load demands of node d in time period t (MW)
$\bar{p}_i, \underline{p}_i$	Upper and lower bounds of power generation of unit i (MW)
RU_i, RD_i	Upward and downward ramping rates of unit i (MW/min)
t	Index of time periods
T	Number of time periods
$\bar{w}_{j,t}, \underline{w}_{j,t}$	The maximum and minimum forecasting power outputs of REG j in time period t (MW)
$\bar{W}_t, \underline{W}_t$	The maximum and minimum forecasting values of the total REG power output in time period t (MW)

B. Functions

$CF_{i,t}(\cdot)$	Fuel cost of unit i in time period t
$E(\cdot)$	Expectation of random variables
$\Phi(\zeta)$	Cumulative distribution function (CDF) of random variable ζ

Manuscript received: August 18, 2022; revised: November 9, 2022; accepted: February 9, 2023. Date of CrossChecked: February 9, 2023. Date of online publication: April 10, 2023.

This work was supported in part by the S&T Project of State Grid Corporation of China (No. 5100-202199512A-0-5-ZN) "Learning based Renewable Cluster Control and Coordinated Dispatch".

S. Xu , W. Wu (corresponding author), B. Wang, and Y. Yang are with the State Key Laboratory of Power Systems, Department of Electrical Engineering, Tsinghua University, Beijing 100084, China, and Y. Yang is also with the School of Electrical Engineering and Automation, Hefei University of Technology, Hefei 230009, China (e-mail: xsw_thu@qq.com; wuwench@tsinghua.edu.cn; wb1984@tsinghua.edu.cn; yangyuethu@foxmail.com).

DOI: 10.35833/MPCE.2022.000526

$\hat{\Phi}(\zeta)$	Approximated CDF of random variable ζ
$\varphi(\zeta)$	Probability density function (PDF) of random variable ζ
$\hat{\varphi}(\zeta)$	Approximated PDF of random variable ζ
$\varphi_t(\tilde{W}_t)$	PDF of random variable $\tilde{W}_t$
$VaR_{1-\beta}\{\cdot\}$	VaR measurements with probability 1–β

C. Deterministic Variables

$\ell_{l,t}$	Scheduled power flow on transmission line l in time period t (MW)
$p_{i,t}$	Scheduled power generation of unit i in time period t (MW)
Q_t^{up}, Q_t^{dn}	Allowable upper and lower bounds of summation of REG output (MW)
$Ru_{i,t}, Rd_{i,t}$	Available upward and downward reserve capacities of unit i in time period t
$w_{j,t}$	Scheduled reference output of REG j in time period t (MW)
W_t	Summation of total scheduled REG output in time period t (MW)

D. Random Variables

$\tilde{\ell}_{l,t}$	Actual power flow on transmission line l in time period t (MW)
$\Delta\tilde{\ell}_{l,t}$	Power deviation from scheduled points on transmission line l in time period t (MW)
$\tilde{w}_{j,t}$	Actual power output of REG j in time period t (MW)
$\tilde{W}_t$	Summation of the total actual REG power output in time period t (MW)

I. Introduction

EXPLOITING and utilizing renewable energy is currently the most practicable measure to tackle climate change issue and fulfil the goal of carbon neutrality. In 2035, the installed wind power and photovoltaic will exceed 1500 GW in China, which accounts for more than half of the total generation capacity [1], [2]. However, the growing penetration of renewable energy generation (REG) results in a more frequent and significant power fluctuation of the net load curve, and thus increases the operational risks of power systems. Chance-constrained probabilistic dispatch is able to cope with generation uncertainty but usually ignores the low-probability events that represent renewable energy curtailment or load shedding. Since the scenarios of insufficient power supply or regulation capability may occur occasionally, the renewable energy curtailment and load shedding should be involved in dispatch stage to make a tradeoff between the reserve regulation and emergency control process. Moreover, the power dispatch that contains multidimensional correlated statistical information is generally modeled as a complicated stochastic dynamic programming. Exploiting computationally efficient algorithm is still a critical issue in real application.

Robust optimization (RO) is recognized as an effective approach to handle the uncertainty of REG. In recent literature, interval RO [3], adjustable RO [4], and two-stage RO [5] have been extensively studied to address generation schedule [3], decentralized power dispatch [5], and unit commitment (UC) [4] problems. These models are generally transformed into tractable problems via dual theory and are able to ensure the operational security for any realization of uncertainties. However, due to the strong randomness with large-scale REG penetration, the solution of RO is likely to be overly conservative, which results in a huge amount of extra reserve adjustable cost.

Stochastic optimization (SO) tends to overcome the drawbacks of RO and achieves a statistical minimization of operating cost under the premise of pre-defined security level. Reference [6] studies a hybrid stochastic/deterministic UC problem in which the allowable range of net load ramping is highlighted via probabilistic constraints. References [7] and [8] propose a chance-constrained economic dispatch (CCED) model with non-Gaussian uncertainty, where the reserve and power flow restrictions are constructed as chance constraints. Day-ahead energy and reserve joint dispatch with multistage REG uncertainties described by scenario trees is developed in [9]. Reference [10] calculates the schedule of devices in microgrids by a two-stage SO model, which coordinates the main grid and multiple microgrids in a decentralized manner. Most of the previous stochastic dispatch models allow operators to ignore the influence of the events with low probability, i.e., the tail part of the REG distribution. However, it is reported that these tails hold important reliability information [11] and indicate the cost of emergency control. If the influence of the potential emergency control strategies, such as renewable energy curtailment/load shedding, is not considered in dispatch model, there will be more operational risks and corrective cost in real-time control stage. Since the shortage of regulation capability occurs frequently in high-renewable power systems, the cost of reserve regulation and renewable energy curtailment/load shedding should be co-optimized in dispatch stage to produce more effective reserve decisions.

Stochastic economic dispatch (SED) that considers expected operational cost is generally a nonlinear programming (NLP) problem with non-analytical objective functions, which prevents the application of SED to practical engineering. Scenario-based approach [12], [13] is tractable by calculating the weighted sum of discrete distributions, but can bring huge computational burden. Reference [14] proposes a piece-wise linearization method to approximate the integral cost terms and transform stochastic UC into a deterministic mixed-integer linear programming (MILP). Sequential linear programming (SLP) is the most popular algorithm to handle SED [7], [8] with expected objective functions. It linearizes the original problem in the neighborhood of the current solution and solves a sequence of linear programming (LP) problems to approach the optimal solution. Unfortunately, the SLP cannot utilize the second-order information and is actually very slow when the solution is not at a vertex [15]. Moreover, the global convergence is likely to be destroyed without a proper trust-region radius in iteration process [16]. Thus, the SLP algorithm is unable to provide a stable solution and not suitable in engineering calculation.

Our previous work [17], [18] focuses on the analytical transformation of SED in order to obtain the schedule more efficiently. Reference [17] employs Cauchy distribution to describe the wind power forecast errors (WPFEs) and converts CCED into deterministic problems, which can be solved efficiently. Reference [18] develops a piece-wise quadratic fitting technique to approximate the expectation terms in objective functions, with which SED is reformulated as a mixed-integer quadratic programming (MIQP) problem. Nevertheless, the scalability and efficiency of these methods still need to be further improved for large-scale high-renewable power grids.

This paper aims to address the existing issues concerning practical implementation of SED. A probabilistic energy and reserve dispatch (PERD) model is developed at first, which makes a trade-off between reserve regulation and renewable energy curtailment/load shedding to generate more economic reserve decisions than traditional CCED methods. It is worth mentioning that the consideration of co-dispatching energy and reserve can improve the security and economy of the power system operation. Since the high penetration of renewable energy brings potential risks of power shortage or transmission congestion, the reserve schedules should be developed in advance together with power dispatch to enhance reliability [19]. Meanwhile, the co-dispatch of energy and reserve can minimize the overall operational cost. These facts have been illustrated by the test in provincial power systems in China [19]. Moreover, we propose an analytical reformulation method to ensure a stable and efficient solution of PERD. Numerical results of IEEE test systems and real provincial power systems in China show that the proposed method is more suitable for bulk power systems with high penetration of renewables. In more detail, the contributions of this paper are twofold.

1) A novel PERD model that considers the expected cost of potential emergency control strategies is proposed to account for the impact of low-probability events in the tail part of REG distributions. Compared with the conventional CCED (C-CCED) models in previous studies [7], [8], [17], [20], the renewable energy curtailment and load shedding are also minimized in dispatch stage to make a tradeoff between reserve regulation and emergency control process, which produces more economic reserve decisions and fully hedge against the strong uncertainties of REG. Since the proposed PRED model specifies the solution of SED to handle the risk scenarios and balance various kinds of cost in reserve scheduling, it is more suitable for practical application than C-CCED in a high-renewable power grid.

2) An analytical reformulation method for PERD is proposed in this paper. Firstly, the expected cost of reserve regulation and emergency control is accurately approximated by analytical functions, which makes the model convex. Secondly, the deterministic transformation of probabilistic constraints is transformed into an unconstrained optimization problem by introducing value-at-risk (VaR) representation. Then, VaR terms are calculated by a computationally-cheap dichotomy search algorithm. Thus, the PERD can be converted into a deterministic and convex problem. Besides, compared to the commonly-used SLP algorithm, the proposed model can be solved more reliably and efficiently with off-the-shelf solvers.

The remainder of this paper is organized as follows. Section II presents the detailed proposed PERD model and discusses the difference between C-CCED models and the proposed PERD model in reserve determination. The reformulation and solution of the proposed PERD model are given in Section III. Section IV shows the case studies, and Section V concludes this paper.

II. Proposed PERD Model and Discassion

In this section, we firstly discuss the detailed objective functions and system constraints of the proposed PERD model in Section II-A and II-B, respectively. Then, the difference in reserve decisions between C-CCED models and the proposed PERD model is clarified in Section II-C.

A. Objective Functions

The PERD model minimizes the total expected operational cost to achieve probabilistic optimality, i.e.,

$$\begin{aligned}\min F = &\sum_{t=1}^{T}\sum_{i=1}^{N} CF_{i,t}\left(p_{i,t}\right) + C_{DN}\sum_{t=1}^{T} E\left(\tilde{W}_t - W_t \middle| W_t \le \tilde{W}_t \le \bar{W}_t\right) + \\ &C_{UP}\sum_{t=1}^{T} E\left(W_t - \tilde{W}_t \middle| \underline{W}_t \le \tilde{W}_t \le W_t\right) + \\ &C_{CUR}\sum_{t=1}^{T} E\left(\tilde{W}_t - Q_t^{up} \middle| Q_t^{up} \le \tilde{W}_t \le \bar{W}_t\right) + \\ &C_{LD}\sum_{t=1}^{T} E\left(Q_t^{dn} - \tilde{W}_t \middle| \underline{W}_t \le \tilde{W}_t \le Q_t^{dn}\right)\end{aligned} \tag{1}$$

where the second and third terms denote downward and upward reserve adjustment costs, respectively; the last two terms represent the emergency control cost of renewable energy curtailment and load shedding, respectively. C_{DN}, C_{UP}, C_{CUR}, and C_{LD} are the corresponding cost coefficients, satisfying $C_{LD} \ge C_{CUR} \ge C_{DN} = C_{UP}$. The capital letters $\tilde{W}_t$, W_t, $\bar{W}_t$, $\underline{W}_t$, Q_t^{up}, and Q_t^{dn} are the summation of the relevant vectors, whose expressions are:

$$\begin{cases}\tilde{W}_t = \sum_{j=1}^{J} \tilde{w}_{j,t} \\ W_t = \sum_{j=1}^{J} w_{j,t} \\ \bar{W}_t = \sum_{j=1}^{J} \bar{w}_{j,t} \\ \underline{W}_t = \sum_{j=1}^{J} \underline{w}_{j,t}\end{cases} \tag{2}$$

$$\begin{cases}Q_t^{up} = W_t + \sum_{i=1}^{N} Rd_{i,t} \\ Q_t^{dn} = W_t - \sum_{i=1}^{N} Ru_{i,t}\end{cases} \tag{3}$$

Each part of (1) is presented in detail as follows.

1) Fuel Cost of Thermal Units

$$CF_{i,t}\left(p_{i,t}\right) = a_i p_{i,t}^2 + b_i p_{i,t} + c_i \tag{4}$$

Equation (4) is a quadratic function of the scheduled generation.

2) Reserve Adjustment Cost

$$E\left(\tilde{W}_t - W_t \middle| W_t \le \tilde{W}_t \le \bar{W}_t\right) = \int_{W_t}^{Q_t^{up}} \left(\tilde{W}_t - W_t\right)\varphi_t\left(\tilde{W}_t\right)\mathrm{d}\tilde{W}_t + \int_{Q_t^{up}}^{\bar{W}_t} \left(Q_t^{up} - W_t\right)\varphi_t\left(\tilde{W}_t\right)\mathrm{d}\tilde{W}_t \quad (5)$$

$$E\left(W_t - \tilde{W}_t \middle| \underline{W}_t \le \tilde{W}_t \le W_t\right) = \int_{Q_t^{dn}}^{W_t} \left(W_t - \tilde{W}_t\right)\varphi_t\left(\tilde{W}_t\right)\mathrm{d}\tilde{W}_t + \int_{\underline{W}_t}^{Q_t^{dn}} \left(W_t - Q_t^{dn}\right)\varphi_t\left(\tilde{W}_t\right)\mathrm{d}\tilde{W}_t \quad (6)$$

Equations (5) and (6) represent the expected downward and upward power regulation costs, respectively.

3) Emergency Control Cost

$$E\left(\tilde{W}_t - Q_t^{up} \middle| Q_t^{up} \le \tilde{W}_t \le \bar{W}_t\right) = \int_{Q_t^{up}}^{\bar{W}_t} \left(\tilde{W}_t - Q_t^{up}\right)\varphi_t\left(\tilde{W}_t\right)\mathrm{d}\tilde{W}_t \quad (7)$$

$$E\left(Q_t^{dn} - \tilde{W}_t \middle| \underline{W}_t \le \tilde{W}_t \le Q_t^{dn}\right) = \int_{\underline{W}_t}^{Q_t^{dn}} \left(Q_t^{dn} - \tilde{W}_t\right)\varphi_t\left(\tilde{W}_t\right)\mathrm{d}\tilde{W}_t \quad (8)$$

Equations (7) and (8) describe the emergency control cost of renewable energy curtailment and load shedding, respectively. In extreme scenarios, the REG output is beyond the manageable range $[Q_t^{dn}, Q_t^{up}]$ and the system operational constraints are violated. Emergency control strategies of renewable energy curtailment and load shedding are required to cope with the power fluctuation and maintain the operational security.

B. System Constraints

1) Power Balance Constraints

$$\sum_{i=1}^{N} p_{i,t} + W_t = \sum_{d=1}^{D} p_{d,t} \quad t = 1, 2, \ldots, T \quad (9)$$

Equation (9) provides basic points to maintain power balance of the system. Any fluctuation of load or REG output should be offset around the scheduled curve.

2) Generation Limit Constraints

$$\underline{p}_i \le p_{i,t} \le \bar{p}_i \quad i = 1, 2, \ldots, N, t = 1, 2, \ldots, T \quad (10)$$

$$\underline{w}_{j,t} \le w_{j,t} \le \bar{w}_{j,t} \quad j = 1, 2, \ldots, J, t = 1, 2, \ldots, T \quad (11)$$

$$0 \le Ru_{i,t} \le \min\left\{\bar{p}_i - p_{i,t}, RU_i \cdot \Delta T\right\} \quad i = 1, 2, \ldots, N, t = 1, 2, \ldots, T \quad (12)$$

$$0 \le Rd_{i,t} \le \min\left\{p_{i,t} - \underline{p}_i, RD_i \cdot \Delta T\right\} \quad i = 1, 2, \ldots, N, t = 1, 2, \ldots, T \quad (13)$$

Constraints (10) and (11) restrict the power generation of thermal units and REGs within a reachable bound, respectively. Constraints (12) and (13) confine the ranges of upward and downward reserve capacities, respectively.

3) Ramping Constraint

$$-RD_i \cdot \Delta T \le p_{i,t} - p_{i,t-1} \le RU_i \cdot \Delta T \quad i = 1, 2, \ldots, N, t = 2, 3, \ldots, T \quad (14)$$

Constraint (14) indicates the incremental output of thermal units between adjacent periods is constrained by their ramping rates.

4) Probabilistic Constraints of Reserve Demand

$$\mathbb{P}\left\{\sum_{i=1}^{N} Ru_{i,t} \ge W_t - \tilde{W}_t\right\} \ge 1 - \beta \quad t = 1, 2, \ldots, T \quad (15)$$

$$\mathbb{P}\left\{\sum_{i=1}^{N} Rd_{i,t} \ge {}_i\tilde{W}_t - W_t\right\} \ge 1 - \beta \quad t = 1, 2, \ldots, T \quad (16)$$

Constraints (15) and (16) ensure that the negative and positive power fluctuations are offset by the preserved upward and downward reserve regulation capacities, respectively, with an acceptable probability $1-\beta$.

5) Probabilistic Constraints of Transmission Security

$$\tilde{\ell}_{l,t} = \sum_{i=1}^{N} G_{l,i}\left[p_{i,t} - \gamma_i\left(\tilde{W}_t - W_t\right)\right] + \sum_{j=1}^{J} G_{l,j}\tilde{w}_{j,t} + \sum_{d=1}^{D} G_{l,d}\, p_{d,t} \quad l = 1, 2, \ldots, L, t = 1, 2, \ldots, T \quad (17)$$

$$\mathbb{P}\left\{\tilde{\ell}_{l,t} \le \bar{L}_l\right\} \ge 1 - \beta \quad l = 1, 2, \ldots, L, t = 1, 2, \ldots, T \quad (18)$$

$$\mathbb{P}\left\{\underline{L}_l \le \tilde{\ell}_{l,t}\right\} \ge 1 - \beta \quad l = 1, 2, \ldots, L, t = 1, 2, \ldots, T \quad (19)$$

Constraints (18) and (19) mean that the actual power flow on transmission line l is limited by its transmission capacity with probability $1-\beta$.

It is noted that the constraints of transmission security are constructed as individual chance constraints rather than two-side chance constraints in this paper. This is because the sending end and receiving end of transmission lines are generally determinated in a specific dispatch period. Simultaneous overloading of forward and backward power flows is almost impossible.

C. Discussion of Proposed PERD Model and C-CCED Models

The proposed PERD model improves C-CCED models in reserve decision procedure. The costs of renewable energy curtailment and load shedding are incorporated in the proposed PERD model to fully account for model the disadvantages of low-probability events. The PERD model allows operators to make a trade-off between emergency control and reserve regulation. By contrast, the influence of the tail part of REG distributions is ignored in C-CCED models [7], [8], [17], [20], which may result in unreasonable scheduled points and exorbitant emergency control cost in real-time stage.

An intuitive comprehension is shown in Fig. 1, where P_{sche} is the scheduled point; and $\underline{P}_{adj}$ and $\bar{P}_{adj}$ are the allowable lower and upper bounds of the REG, respectively. We use black lines to describe the solution of the proposed PERD model, in which reserve regulation is employed to offset the small power fluctuations, and the emergency control of renewable energy curtailment and load shedding is implemented when the power output of REG is outside the interval $[\underline{P}_{adj}, \bar{P}_{adj}]$. With the optimal objective (1), the proposed PERD model can realize a balance between reserve regulation costs and emergency control cost, and thus achieves an efficient utilization of reserve resources. For comparison, the

solution of C-CCED models is depicted by red lines in Fig. 1. Since the cost price of load shedding is ignored, the scheduled point of C-CCED models [7], [8], [17] is likely to be larger than the proposed PERD model. Correspondingly, the reserve regulation range is shifted to a higher position. In this case, the load shedding which is more expensive than renewable energy curtailment covers more risk scenarios than the proposed PRED model. Thus, the corrective burden will be increased in real-time control stage with C-CCED models, which results in more emergency control cost and thus more operational cost.

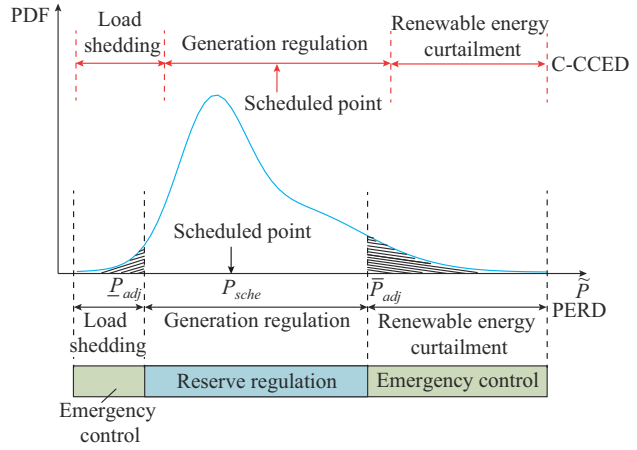

Fig. 1. Comparison of C-CCED and proposed PERD models.

III. Reformulation and Solution of Proposed PERD Model

In this section, we firstly discuss the convexity of the objective function, in which the expectation terms are reformulated analytically by an approximation technique. Then, we propose a deterministic transformation method of probabilistic constraints based on the VaR formulas. Finally, the solution of the proposed PERD model is given.

A. Assumption

Considering that any smooth PDF can be approximated precisely by Gaussian mixture model (GMM) with enough Gaussian components and specific parameters [21], a multi-dimensional GMM is employed to construct the joint distribution of the power output of all REGs in time period t, i.e., $\tilde{\boldsymbol{w}}_t$. The PDF can be written as:

$$\varphi_t\left(\tilde{\boldsymbol{w}}_t\right)=\sum_{m=1}^{M}\omega_{t,m}\varphi_{t,m}\left(\tilde{\boldsymbol{w}}_t\middle|\boldsymbol{\mu}_{t,m},\boldsymbol{\Sigma}_{t,m}\right) \tag{20}$$

$$\begin{cases}\omega_{t,m}\geq 0\\ \sum_{m=1}^{M}\omega_{t,m}=1\end{cases} \tag{21}$$

where $\varphi_{t,m}(\cdot)$ is the PDF of a Gaussian distribution with expectation vector $\boldsymbol{\mu}_{t,m}$ and covariance matrix $\boldsymbol{\Sigma}_{t,m}$.

Generally, the construction of GMM is accomplished in the probability forecasting stage, which is a fitting process integrating the latest numeric weather prediction and large amount of historical data [22], [23]. The expectation maximization (EM) algorithm is commonly used to estimate the parameters in (20).

B. Analytical Approximation of Objective Functions

The convexity of the objective function is firstly illustrated in this subsection. We define an integral function to calculate the part over a baseline of the PDF.

$$E_{ep}\left(x\middle|\underline{x}\right)=\int_{\underline{x}}^{x}(x-v)\varphi(v)\mathrm{d}v \tag{22}$$

where v is a GMM random variable with PDF $\varphi(v)$; and $\underline{x}$ is a constant. It is observed that $E_{ep}\left(x\middle|\underline{x}\right)$ is a convex function in $\mathbb{R}$ because the second-order derivative is nonnegative, i.e.,

$$\frac{\partial^2}{\partial x^2}E_{ep}\left(x\middle|\underline{x}\right)=\varphi(x)>0 \tag{23}$$

Let $F_{C,t}\left(W_t,Q_t^{up},Q_t^{dn}\right)$ denote the total reserve adjustment and emergency control cost in time period t. Combined with (22), we have

$$\begin{aligned}F_{C,t}\left(W_t,Q_t^{up},Q_t^{dn}\right)=&C_{DN}E_{ep}\left(W_t\middle|\bar{W}_t\right)+C_{UP}E_{ep}\left(W_t\middle|\underline{W}_t\right)+\\&\left(C_{CUR}-C_{DN}\right)E_{ep}\left(Q_t^{up}\middle|\bar{W}_t\right)+\left(C_{LD}-C_{UP}\right)E_{ep}\left(Q_t^{dn}\middle|\underline{W}_t\right)\end{aligned} \tag{24}$$

Thus, the Hessian matrix of $F_{C,t}\left(W_t,Q_t^{up},Q_t^{dn}\right)$ can be derived as:

$$\boldsymbol{H}\left(F_{C,t}\left(W_t,Q_t^{up},Q_t^{dn}\right)\right)=\begin{bmatrix}(C_{DN}+C_{UP})\varphi(W_t) & 0 & 0\\ 0 & (C_{CUR}-C_{DN})\varphi(Q_t^{up}) & 0\\ 0 & 0 & (C_{LDN}-C_{UP})\varphi(Q_t^{dn})\end{bmatrix} \tag{25}$$

Since the unit renewable energy curtailment or load shedding cost is larger than the unit downward or upward reserve adjustment cost, (25) is positive definite. Therefore, the objective function (1) is convex with respect to W_t, Q_t^{up}, and Q_t^{dn}.

Then, we propose an approximation technique to handle the objective function analytically. The major challenge is that the expectation terms in (24) cannot be calculated directly with off-the-shelf optimization solvers. SLP has been widely used in relevant studies [7], [8], [24], which linearize the cost function and find the optimization solution iteratively. However, in some cases, SLP is inefficient and even diverges [18], which limits the application of SLP in practical engineering. For convenience, we first rewrite the integral function (22) as:

$$\begin{aligned}E_{ep}\left(x\middle|\underline{x}\right)=&\sum_{m=1}^{M}\omega_m\left[\left(x-\mu_m\right)\Phi_m(x)+\sigma_m^2\varphi_m(x)\right]-\\&x\Phi\left(\underline{x}\right)+\sum_{m=1}^{M}\omega_m\left(\mu_m\Phi_m\left(\underline{x}\right)-\sigma_m^2\varphi_m\left(\underline{x}\right)\right)\end{aligned} \tag{26}$$

where $\varphi_m(\cdot)$ and $\Phi_m(\cdot)$ are the PDF and cumulative distribution function (CDF) of the m^{th} Gaussian component, respectively, with the weight coefficient ω_m, expectation μ_m, and standard deviation σ_m.

Our previous work [25] develops a composite hyperbolic tangent function to approach the CDF of GMM, based on

which, the CDF and PDF of Gaussian distribution with expectation μ and standard deviation σ can be approximated as:

$$\begin{cases} \Phi_0\left(x\,|\,\mu,\sigma\right) \approx \hat{\Phi}_0\left(x\,|\,\mu,\sigma\right) \\ \varphi_0\left(x\,|\,\mu,\sigma\right) \approx \hat{\varphi}_0\left(x\,|\,\mu,\sigma\right) = \dfrac{\mathrm{d}\hat{\Phi}_0\left(x\,|\,\mu,\sigma\right)}{\mathrm{d}x} \end{cases} \tag{27}$$

where $\hat{\varphi}_0\left(x\,|\,\mu,\sigma\right)$ is the approximated PDF; and $\hat{\Phi}_0\left(x\,|\,\mu,\sigma\right)$ is the approximated CDF, whose expression is described by:

$$\hat{\Phi}_0\left(x\,|\,\mu,\sigma\right) = \frac{1}{2} + \frac{1}{2}\tanh\left(0.7983\frac{x-\mu}{\sigma} + 0.03564\left(\frac{x-\mu}{\sigma}\right)^3\right) \tag{28}$$

Therefore, $E_{ep}\left(x\,|\,\underline{x}\right)$ can be estimated as $\hat{E}_{ep}\left(x\,|\,\underline{x}\right)$:

$$\hat{E}_{ep}\left(x\,|\,\underline{x}\right) = \sum_{m=1}^{M}\omega_m\left[\left(x-\mu_m\right)\hat{\Phi}_m\left(x\right) + \sigma_m^2\hat{\varphi}_m\left(x\right)\right] - x\hat{\Phi}\left(\underline{x}\right) + \sum_{m=1}^{M}\omega_m\left(\mu_m\hat{\Phi}_m\left(\underline{x}\right) - \sigma_m^2\varphi_m\left(\underline{x}\right)\right) \tag{29}$$

Equation (29) is analytical without any integral terms. Considering that $\hat{\Phi}_0\left(x\,|\,\mu,\sigma\right)$ maintains the continuity, monotonicity, differentiability, and convexity of $\Phi_0\left(x\,|\,\mu,\sigma\right)$, (29) is also convex with respect to variable x. The proof of convexity of (29) is given in Appendix A.

C. Deterministic Transformation of Probabilistic Constraints

For simplicity, we use (30) to represent the probabilistic constraints in the proposed PERD model uniformly. According to the VaR theory, (30) can be converted into VaR constraint (31) equivalently.

$$\mathbb{P}\left\{\tilde{y}+f\left(\boldsymbol{x}\right)\le g\left(\boldsymbol{x}\right)\right\}\ge 1-\beta \tag{30}$$

$$VaR_{1-\beta}\left\{\tilde{y}+f\left(\boldsymbol{x}\right)\right\}\le g\left(\boldsymbol{x}\right) \tag{31}$$

where $\tilde{y}$ denotes a random variable; $\boldsymbol{x}$ is a decision vector; $\tilde{y}+f\left(\boldsymbol{x}\right)$ is called loss function in VaR formulas; and $VaR_{1-\beta}\{\cdot\}$ is defined as [26]:

$$VaR_{1-\beta}\left\{\tilde{y}+f\left(\boldsymbol{x}\right)\right\} = \min\left\{\alpha\in\mathbb{R}:\int_{\tilde{y}+f\left(\boldsymbol{x}\right)\le\alpha}\varphi\left(\tilde{y}\right)\mathrm{d}\tilde{y}\ge 1-\beta\right\} \tag{32}$$

Based on the definition of VaR in (32), the deterministic transformation of probabilistic constraints is turned into an unconstrained optimization problem, which can be solved efficiently by one-dimensional search method. In this paper, a dichotomy algorithm is employed to compute the value of $VaR_{1-\beta}\{\cdot\}$ in constraint (31), as demonstrated in Algorithm 1. Especially in *Step 2-2*, the cumulative density can be calculated directly by the proposed approximated function (27) without any integration. Since the sequence generated by dichotomy algorithm is exponentially convergent, Algorithm 1 is actually very efficient.

D. Solution and Discussion

In this subsection, we firstly rewrite the probabilistic constraints in the proposed PERD model into VaR constraints. Reserve demand constraints (15) and (16) can be replaced by (33) and (34), respectively.

Algorithm 1

Calculate the value of $VaR_{1-\beta}\{\cdot\}$ with GMM uncertainty

$$\begin{cases} VaR_{1-\beta}\left\{\tilde{y}+f\left(\boldsymbol{x}\right)\right\} = \min\left\{\alpha\in\mathbb{R}:\int_{\tilde{y}+f\left(\boldsymbol{x}\right)\le\alpha}\varphi\left(\tilde{y}\right)\mathrm{d}\tilde{y}\ge 1-\beta\right\} \\ \tilde{y}\sim GMM\left(\boldsymbol{\omega}_y,\boldsymbol{\mu}_y,\boldsymbol{\sigma}_y\right) \end{cases}$$

1: Separate $f(\boldsymbol{x})$ from $VaR_{1-\beta}\{\tilde{y}+f(\boldsymbol{x})\}$

Let $\lambda=\alpha-f(\boldsymbol{x})$, then

$$VaR_{1-\beta}\left\{\tilde{y}+f\left(\boldsymbol{x}\right)\right\} = \min\left\{\lambda+f\left(\boldsymbol{x}\right):\int_{\tilde{y}\le\lambda}\varphi\left(\tilde{y}\right)\mathrm{d}\tilde{y}\ge 1-\beta\right\} = \min\left\{\lambda:\int_{\tilde{y}\le\lambda}\varphi\left(\tilde{y}\right)d\tilde{y}\ge 1-\beta\right\} + f\left(\boldsymbol{x}\right) = VaR_{1-\beta}\left\{\tilde{y}\right\} + f\left(\boldsymbol{x}\right)$$

2: Calculate the value of $VaR_{1-\beta}\{\tilde{y}\}$

Step 2-1: set a convergence tolerance $\varepsilon>0$; initialize the upper and lower bounds of $VaR_{1-\beta}\{\tilde{y}\}$ as $\bar{V}$ and $\underline{V}$, respectively

Step 2-2: set $V_{1-\beta}\left(\tilde{y}\right)=(\underline{V}+\bar{V})/2$, and solve

$$\theta = \int_{\tilde{y}\le V_{1-\beta}\left(\tilde{y}\right)}\varphi_y\left(\tilde{y}\right)\mathrm{d}\tilde{y} = \sum_{m=1}^{M}\omega_{y,m}\hat{\Phi}_{y,m}\left(V_{1-\beta}\left(\tilde{y}\right)\middle|\,\mu_{y,m},\sigma_{y,m}\right)$$

Step 2-3: if $\theta>1-\beta$, update $\bar{V}=V_{1-\beta}\left(\tilde{y}\right)$; else update $\underline{V}=V_{1-\beta}\left(\tilde{y}\right)$

Step 2-4: if $\bar{V}-\underline{V}\le\varepsilon$, terminate and obtain $VaR_{1-\beta}\{\tilde{y}\}=V_{1-\beta}\left(\tilde{y}\right)$; else go to *Step 2-2*

3: Obtain the expression of $VaR_{1-\beta}\{\tilde{y}+f(\boldsymbol{x})\}$

$VaR_{1-\beta}\left\{\tilde{y}+f\left(\boldsymbol{x}\right)\right\} = V_{1-\beta}\left(\tilde{y}\right)+f\left(\boldsymbol{x}\right)$

$$VaR_{1-\beta}\left\{W_t-\tilde{W}_t\right\}\le\sum_{i=1}^{N}Ru_{i,t}\quad t=1,2,\ldots,T \tag{33}$$

$$VaR_{1-\beta}\left\{\tilde{W}_t-W_t\right\}\le\sum_{i=1}^{N}Rd_{i,t}\quad t=1,2,\ldots,T \tag{34}$$

In (33) and (34), the negative and positive power fluctuations that result in upward and downward reserve regulation are defined as loss functions. Similarly, the transmission security constraints (18) and (19) are equivalent to (35)-(38).

$$\ell_{l,t}=\sum_{i=1}^{N}G_{l,i}p_{i,t}+\sum_{j=1}^{J}G_{l,j}w_{j,t}+\sum_{d=1}^{D}G_{l,d}p_{d,t}\quad l=1,2,\ldots,L,t=1,2,\ldots,T \tag{35}$$

$$\Delta\tilde{\ell}_{l,t}=\tilde{\ell}_{l,t}-\ell_{l,t}=-\sum_{i=1}^{N}G_{l,i}\gamma_i\left(\tilde{W}_t-W_t\right)+\sum_{j=1}^{J}G_{l,j}\left(\tilde{w}_{j,t}-w_{j,t}\right)\quad l=1,2,\ldots,L,t=1,2,\ldots,T \tag{36}$$

$$VaR_{1-\beta}\left\{\Delta\tilde{\ell}_{l,t}\right\}\le\bar{L}_l-\ell_{l,t}\quad l=1,2,\ldots,L,t=1,2,\ldots,T \tag{37}$$

$$VaR_{1-\beta}\left\{-\Delta\tilde{\ell}_{l,t}\right\}\le\ell_{l,t}-\underline{L}_l\quad l=1,2,\ldots,L,t=1,2,\ldots,T \tag{38}$$

The power flow deviations from the scheduled points in two directions are defined as the loss functions in (37) and (38).

According to Algorithm 1, constraints (33), (34), (37), and (38) are equivalent to the following deterministic constraints.

$$V_{1-\beta}\left(-\tilde{W}_t\right)+W_t\le\sum_{i=1}^{N}Ru_{i,t}\quad t=1,2,\ldots,T \tag{39}$$

$$V_{1-\beta}\left(\sum_{j=1}^{J}\left(G_{l,j}-\sum_{i=1}^{N}G_{l,i}\gamma_i\right)\tilde{w}_{j,t}\right)-\sum_{j=1}^{J}\left(G_{l,j}-\sum_{i=1}^{N}G_{l,i}\gamma_i\right)w_{j,t}\le\bar{L}_l-\ell_{l,t}\quad l=1,2,\ldots,L,t=1,2,\ldots,T \tag{40}$$

$$V_{1-\beta}\left(\sum_{j=1}^{J}\left(\sum_{i=1}^{N}G_{l,i}\gamma_i-G_{l,j}\right)\tilde{w}_{j,t}\right)+\sum_{j=1}^{J}\left(G_{l,j}-\sum_{i=1}^{N}G_{l,i}\gamma_i\right)w_{j,t}\le\ell_{l,t}-\underline{L}_l$$
$$l=1,2,\ldots,L,t=1,2,\ldots,T \quad (41)$$

On the basis of the above formulation, the original PERD model is transformed to a deterministic problem as (42).

$$\begin{cases}\min F=\\ \quad\sum_{t=1}^{T}\sum_{i=1}^{N}CF_{i,t}\left(p_{i,t}\right)+C_{DN}\sum_{t=1}^{T}\hat{E}_{ep}\left(W_t\middle|\bar{W}_t\right)+C_{UP}\sum_{t=1}^{T}\hat{E}_{ep}\left(W_t\middle|\underline{W}_t\right)+\\ \quad\left(C_{CUR}-C_{DN}\right)\sum_{t=1}^{T}\hat{E}_{ep}\left(Q_t^{up}\middle|\bar{W}_t\right)+\left(C_{LD}-C_{UP}\right)\sum_{t=1}^{T}\hat{E}_{ep}\left(Q_t^{dn}\middle|\underline{W}_t\right)\\ \text{s.t. (9)-(14), (39)-(41)}\end{cases} \quad (42)$$

Since (42) is convex and can be efficiently solved by off-the-shelf solvers, the proposed PERD model is actually very suitable to real applications.

IV. Numerical Tests

Case studies are carried out on a modified IEEE 39-bus system and a provincial power system in China. The former experiment is performed to verify the effectiveness of the proposed method, and also analyze the advantages over pervious schemes in terms of security, economy, and solving efficiency. The latter experiment is conducted on an existing power system with large-scale wind power integration to demonstrate the practical merits of the proposed method. The modified IEEE test system adopted in Section IV-A to IV-E contains 46 branches, 10 thermal units, and 3 wind farms (whose capacities are 250 MW, 300 MW, and 300 MW, respectively). The marginal probability distributions of the power output of all wind farms are acquired from the probabilistic prediction system in Northeast China. Nataf transformation is employed to generate correlated data samples in each period [20], which are fitted into a two-component joint GMM with EM algorithm. Specifically, the probabilistic forecasts of the total wind power output ($\Delta T=1$ hour) are shown in Fig. 2. Other detailed information of the test data can be found in [27]. Besides, the parameters of the practical power system are reported in Section IV-F.

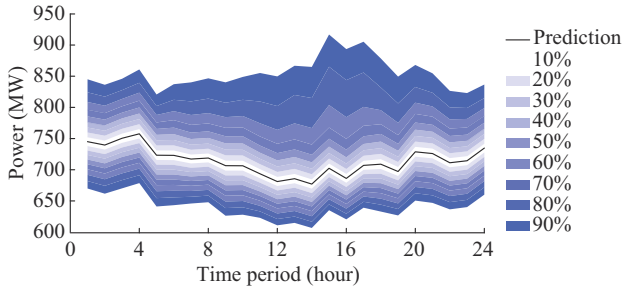

Fig. 2. Probabilistic forecasts of total wind power output.

The following tests conduct PERD for 24 hours with a 1-hour resolution. The confidence level is set to be 0.9. For simplicity, the participation factor of each unit is proportional to its capacity. In addition, the unit cost of upward/downward power adjustment is set to be 50 $/MW. The cost coefficients of wind curtailment and load shedding are assumed to be 100 $/MW and 200 $/MW, respectively. All simulations are performed on a personal computer with 2.30-GHz Intel Core i7 and 16 GB RAM. The program environment is MATLAB 2018a. PERD is solved by IPOPT, while other models for comparison are handled with solver Gurobi 9.1.0.

A. Dispatch Result Analysis and Approximation Accuracy Verification

The dispatch results of the total wind farm output are depicted in Fig. 3, which can be comprehended from two aspects. On the one hand, the scheduled curve builds reference points of the uncertainty generation to participate in the power balance scheme. It varies slightly around the predicted curve in Fig. 2 to avoid the expensive reserve adjustment cost. On the other hand, PERD provides allowable upper and lower bounds of the random generation, which establishes a trade-off between reserve adjustment and emergency control costs actually. Power fluctuations out of the allowable threshold will be offset by wind curtailment or load shedding procedure, as shown by the red curve in Fig. 3. In addition, the distribution of the potential wind curtailment and load shedding is presented in Fig. 4, which demonstrates that the low-probability events in tail parts are sufficiently considered in the proposed PERD model.

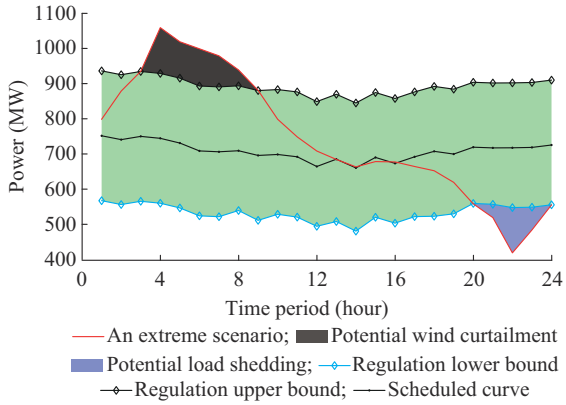

Fig. 3. Dispatch results of total wind power output.

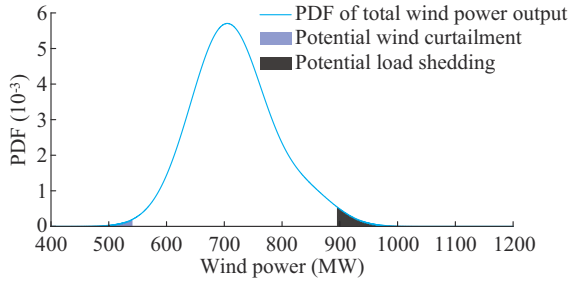

Fig. 4. PDF of potential wind curtailment and load shedding at 08:00.

To verify the effectiveness of the proposed analytical model (42), we analyze the approximation error of the objective function. For the sake of explanation, the relative error *RE* is defined as:

$$RE=\frac{\left|\hat{F}_{C,t}-F_{C,t}\right|}{F_{C,t}} \quad t=1,2,\ldots \quad (43)$$

Figure 5 shows the cost curves and their error in 24 peri-

ods, from which we can find that the relative error between the true values and the approximate solution is in the order of 10^{-4}. Therefore, the proposed approximation method is accurate enough to be applied in practical engineering.

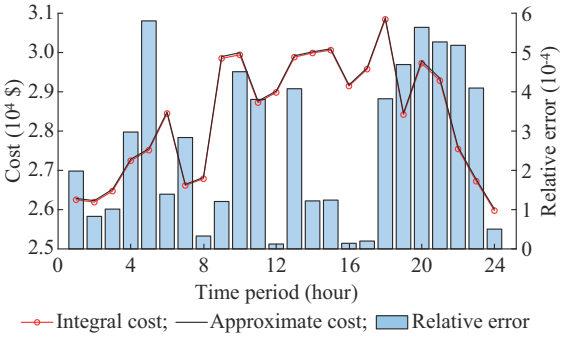

Fig. 5. Cost curves and their error in objective functions.

B. Sensitivity Analysis with Different Cost Coefficients of Wind Curtailment and Load Shedding

This subsection discusses the impact of different cost coefficients (C_{CUR} and C_{LD}) on scheduled results. We increase C_{CUR} uniformly from 100 \$/MW to 300 \$/MW with intervals of 50 \$/MW and define the unit cost proportion *UCP* to represent the relative values of C_{CUR} and C_{LD}, as shown in (44). Then, the ratio of total wind curtailment and load shedding in each case, that is defined as *CLR* in (45), is presented in Fig. 6.

$$UCP = \frac{C_{CUR}}{C_{LD}} \tag{44}$$

$$CLR = \frac{\sum_{t=1}^{T} E\left(\tilde{W}_t - Q_t^{up} \middle| Q_t^{up} \le \tilde{W}_t \le \bar{W}_t\right)}{\sum_{t=1}^{T} E\left(Q_t^{dn} - \tilde{W}_t \middle| \underline{W}_t \le \tilde{W}_t \le Q_t^{dn}\right)} \tag{45}$$

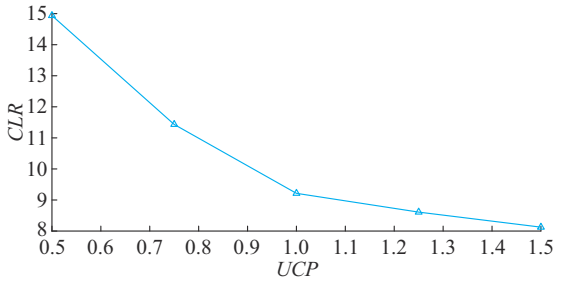

Fig. 6. Ratio of wind curtailment and load shedding with different cost coefficients.

It turns out that *CLR* decreases with the increase of *UCP*. This is because the proposed PERD model will preserve more downward reserve capacities rather than upward reserve capacities when the unit curtailment cost is larger. This experiment allows operators to select appropriate cost coefficients to properly allocate the amount of reserve in two directions. Generally, the pricing of wind curtailment/load shedding depends on the market mechanism and operational requirements. The details of pricing methods are beyond the scope of this paper and not discussed here.

C. Comparison with SLP Algorithm

This experiment is carried out to test the computational performance of the proposed method. For comparison, we also solve the proposed PERD model by means of the commonly-used SLP algorithm [7], [8] with different trust-region radiuses Δ, which means the narrowing ratio of the feasible region in iterations. It should be mentioned that the determination of trust-region radius is usually a cut-and-try process. For convenience, Δ is set to be constant here. The implementation of SLP refers to [16]. Table I shows the CPU time along with the optimal total cost in each case. Simultaneously, the iterative process of SLP algorithm with $\Delta = 0.8$ is presented in Fig. 7. It can be concluded that the SLP algorithm has very heavy computational burden although all cases converge. Moreover, the results of the SLP algorithm may converge to a non-optimal solution without an appropriate Δ. By contrast, the proposed analytical model (42) can be solved stably within less than 5 s even with a general open source solver, which is sufficiently acceptable in practical use.

TABLE I
COMPARISON OF PROPOSED METHOD AND SLP WITH DIFFERENT Δ

Case	Iteration	CPU time (s)	Total cost ($)
Proposed method		4.61	1029343.6
SLP with $\Delta = 0.5$	11	18.36	1030601.2
SLP with $\Delta = 0.8$	24	39.42	1029523.7

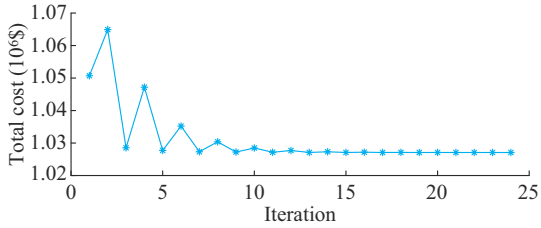

Fig. 7. Iterative process of SLP algorithm.

D. Comparison of Dispatch Results with Different Models

In this subsection, Monte Carlo simulation (MCS) is used to evaluate the solution quality in terms of economy and security. We compared the proposed PERD model with the recently studied dispatch models that consider the uncertainty of wind power, which include:

1) Deterministic ED (D-ED) [28]: the wind power prediction is regarded as the schedule of wind farms to participate in the power balance. The amount of upward/downward reserve is set to be 10% of wind farm capacities.

2) Robust ED (R-ED): the objective function of R-ED is to minimize the summation of generation, wind curtailment, and load shedding costs, subjected to the robust reserve and transmission power flow constraints [3].

3) C-CCED [7]: the objective function of C-CCED contains generation cost and power adjustment cost, i.e., (4)-(6). The confidence level of chance constraints is set to be 0.9.

The simulation results with 100000 scenarios are shown in Table II, where the generation cost is calculated via (4), the reserve adjustable cost and emergency control cost are

the average of all random scenarios, corresponding to (5), (6) and (7), (8), respectively. Total cost is the summation of generation cost, reserve adjustable cost, and emergency control cost. As for the indexes of the satisfaction rate of probabilistic constraints, we firstly calculate the value of $VaR_{1-\beta}\{\cdot\}$ on the left-hand side of constraints (33), (34), (37) and (38) via the sampled discrete distribution. Then, we check whether these probabilistic constraints hold or not for all units/transmission lines in all periods. The satisfaction rate is the ratio of the number of feasible constraints to total constraints.

TABLE II
DISPATCH RESULTS WITH DIFFERENT MODELS

Model	Generation cost ($)	Reserve adjustable cost ($)	Emergency control cost ($)	Total cost ($)	Satisfaction rate (%)	
					Reserve demand constraints	Transmission security constraints
D-ED	949129.6	63484.1	24098.5	1036712.2	79.16	98.09
R-ED	954943.6	85641.8	1005.7	1041591.1	100.00	100.00
C-CCED	953602.9	67814.9	15126.5	1036544.4	100.00	100.00
Proposed PERD	954514.9	71283.9	3544.7	1029343.6	100.00	100.00

It is observed that compared with the proposed PERD model, D-ED/R-ED results in much more emergency control cost or generation cost due to inappropriate allocation of regulation reserves or conservativeness of security constraints. Moreover, although C-CCED achieves the minimization of total generation and reserve adjustable cost, the ignorance of wind curtailment and load shedding brings a considerable amount of emergency control cost. On the other hand, D-ED only realizes the satisfaction rate of reserve demand in 79.16% and transmission security in 98.09%, which cannot meet the operational requirement. On the whole, the proposed PERD model could yield more economic strategies than previous ones under the premise of ensuring the prespecified security level.

E. Comparison with Gaussian Uncertainty

This subsection compares the performance of GMM with Gaussian distribution. Taking wind farm 2 as an example, the marginal PDF of wind power in different periods is illustrated in Fig. 8, where the histogram represents the original distribution of the data samples, and red lines and green lines denote the fitting results of GMM and Gaussian distribution, respectively. Obviously, GMM fits asymmetric and multimodal non-Gaussian distributions more precisely than Gaussian distribution. Subsequently, the proposed PRED is carried out on the modified IEEE 39-bus system with these two distributions.

The dispatch results are tested by MCS in 100000 random scenarios. The average total cost and satisfaction rate of probabilistic constraints are listed in Table III. It is observed that the security level of PERD is unacceptable when inputting Gaussian distributions. Besides, the inaccuracy of Gaussian distribution results in more operational cost than GMM.

F. Comparison with Two-side Chance-constrained Model

The impact of two-side transmission security chance constraints is illustrated in this subsection. In two-side chance-constrained energy and reserve dispatch (TS-CCERD) model, the transmission security chance constraints (18) and (19) are replaced by the two-side chance constraint in (46).

$$\mathbb{P}\left\{\underline{L}_l \le \tilde{\ell}_{l,t} \le \bar{L}_l\right\} \ge 1-\beta \quad l=1,2,\ldots,L, t=1,2,\ldots,T \tag{46}$$

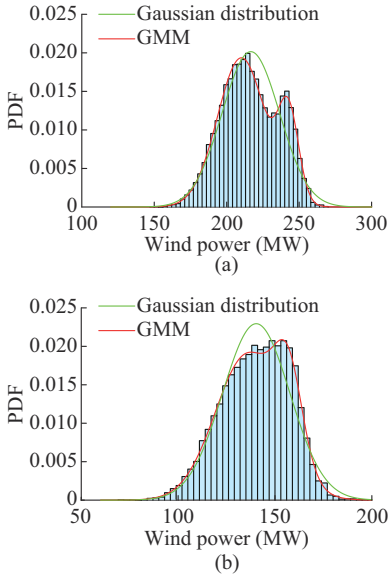

Fig. 8. Marginal PDF of wind power of wind farm 2. (a) At 01:00. (b) At 12:00.

TABLE III
DISPATCH RESULTS WITH GMM AND GAUSSIAN DISTRIBUTION

Model	Total cost ($)	Satisfaction rate (%)	
		Reserve demand constraints	Transmission security constraints
GMM	1029343	100.00	100.00
Gaussian distribution	1031762	91.67	98.09

The solution method of (46) can be found in [29], which provides an inner approximation of two-side chance constraints. Then, the comparison between the proposed PERD and the TS-CCERD models [29] with different transmission capacities and uncertainty models is shown below.

1) With Gaussian Uncertainty

Considering that the approximation method of two-side chance constraints in [29] is exact with Gaussian uncertainty, Gaussian distribution that is fitted in Section IV-E is first used in the dispatch model. We decrease the transmission capacity of line #24 from 200 MW to 75 MW and then carry out the proposed PERD model and the TS-CCERD model in

each case. The total cost and transmission security level considering Gausian uncertainty are shown in Fig. 9. In particular, the security level refers to the ratio of the number of security scenarios to the sampled scenarios. While in security scenarios, the power flow on transmission lines is limited within the upper and lower bounds simultaneously. It is concluded that when the transmission capacity is greater than or equal to 125 MW, the single-side relaxation of chance constraints is exact; in other words, the upper and lower bounds are not violated simultaneously. When the transmission capacity is decreased to 100 MW, the single-side chance constraints are relaxations of two-side ones. While the relaxed gap of confidence level is around 1%, which is actually acceptable in practical use. Besides, when we continue to reduce the capacity of transmission lines, the TS-CCERD model is infeasible.

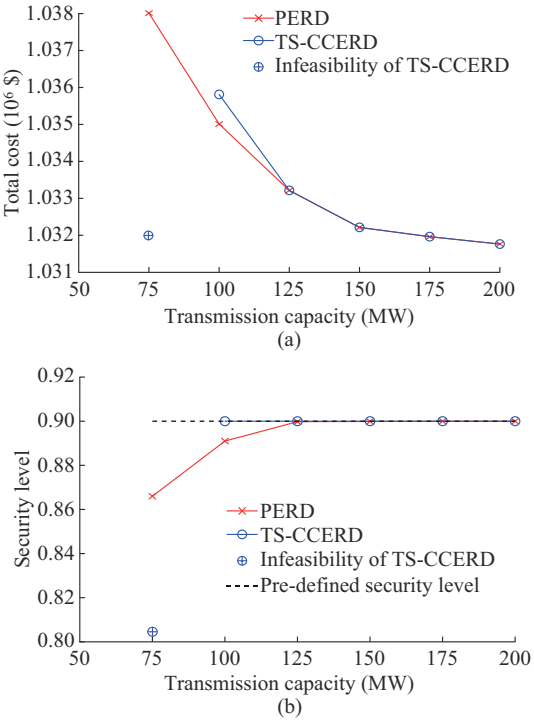

Fig. 9. Total cost and transmission security level with different transmission capacities of line #24 considering Gaussian uncertainty. (a) Total cost. (b) Security level.

2) With GMM Uncertainty

We also compare the PERD model and the TS-CCERD model with GMM uncertainty that is used in Section IV-A to IV-D. In this case, the method presented in [29] only provides an inner approximation of the original two-side chance constraints. The dispatch results are presented in Fig. 10. It is observed that the approximation method in [29] is conservative with respect to dispatch cost and security level, even though the single-side relaxation model is exact when the transmission capacity is greater than or equal to 125 MW. Besides, the approximation method may result in the infeasibility of the TS-CCERD model.

Based on the above discussion, it is concluded that the single-side relaxation of transmission security chance constraints is usually exact except for some extreme cases. In addition, the TS-CCERD model with GMM uncertainty using convex approximation method is conservative and can result in infeasibility. Therefore, the single-side transmission security chance constraints are more applicable in power system practices.

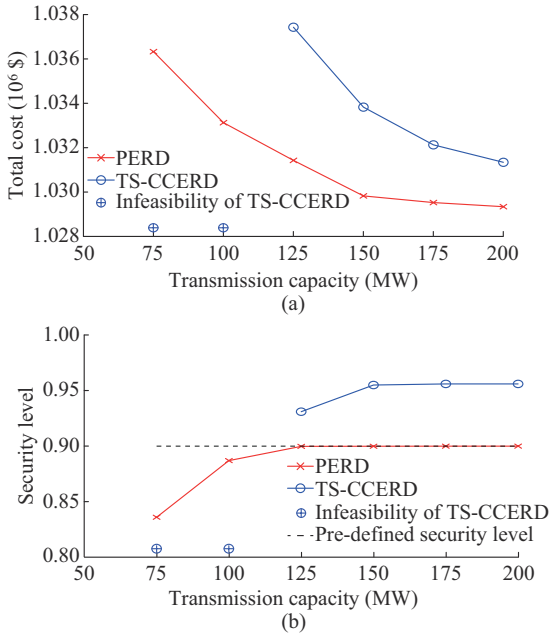

Fig. 10. Total cost and transmission security level with different transmission capacities of line #24 considering GMM uncertainty. (a) Total cost. (b) Security level.

G. Case Studies on Real Power Systems

The proposed PERD model is also implemented on a provincial power system in Northeast China that contains 65 thermal units and 34 wind farms. The detailed information is reported in Table IV. The probabilistic forecasts of the total wind generation are shown in Fig. 11. Other dispatch parameters are set to be consistent with the IEEE test systems.

TABLE IV
SYSTEM SUMMARY OF PROVINCIAL POWER SYSTEM

System	Parameter
Bus	319
Thermal unit	65×19.3 GW
Wind farm	34×5.98 GW
Branch	431

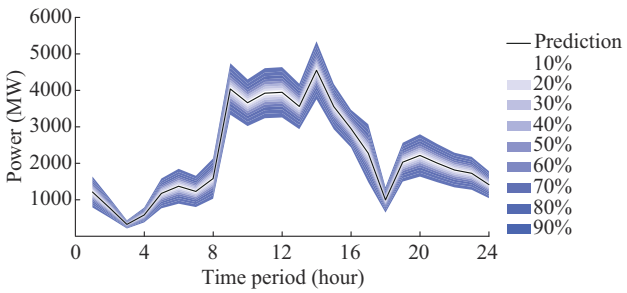

Fig. 11. Probabilistic forecasts of total wind generation.

Firstly, the proposed PERD model is compared with D-ED, R-ED, and C-CCED models in terms of economy and security. MCSs with 100000 wind scenarios are adopted to compute the average total cost and satisfaction rate of probabilistic constraints, which is the same as the previous experiment. The simulation results are listed in Table V. It is observed that the total operation cost with the proposed PERD model is the lowest among all dispatch results. Moreover, compared with D-ED, the proposed PERD model is able to ensure the feasibility of probabilistic constraints and thus guarantee the pre-defined security level. As for the solution efficiency, SLP algorithm converges after 38 iterations with twice the computation time of the proposed analytical method. Therefore, the proposed PERD model and the analytical method are more effective and efficient in practical applications.

TABLE V
SIMULATION RESULTS WITH DIFFERENT MODELS

Item	Model	Result
Total cost (economy)	D-ED	¥272338.3
	R-ED	¥298996.5
	C-CCED	¥273372.5
	Proposed PERD	¥271524.2
Satisfaction rate of probabilistic constraints* (security)	D-ED	92.80%
	Proposed PERD	100.00%
CPU time (efficiency)	SLP ($\Delta = 0.8$)	72.32 s
	Proposed PERD	33.78 s

Note: * means this index is the average of the satisfaction rate of reserve demand and transmission security constraints.

Discussion: based on the test results in two different networks, we can conclude that the proposed PERD model could yield more economic decisions than previous models under the premise of ensuring pre-specified security level regardless of the network type. Although the increasing scale of network results in more computational burden, the solution time of the proposed analytical method is acceptable even for provincial power grids.

V. CONCLUSION

In this paper, we propose a novel PERD model that considers the expected cost of potential emergency control account for the strong uncertainties in a high-renewable power grid. Based on the approximation technique of GMM, the expected costs of reserve regulation and emergency control are accurately re-expressed by analytical functions. Besides, the probabilistic constraints are reformulated by introducing VaR representations, which can be calculated by a computationally-cheap dichotomy search. Thus, the proposed PERD model is converted into a deterministic and convex problem. Case studies performed on IEEE test systems and a provincial power system in China demonstrate that the proposed PERD model could yield more economic decisions than previous models under the premise of ensuring the pre-specified security level. Moreover, compared to the commonly-used SLP algorithm, the proposed PERD model can be solved more reliably and efficiently with off-the-shelf solvers. In our future work, we will further investigate how to distribute the amount of renewable energy curtailment/load shedding between each renewable energy stations/loads fairly.

APPENDIX A

The convexity of (29) is proven as follows.

Let $u = \left(x - \mu_m\right)/\sigma_m$. We define a function $\mathcal{F}_m(u)$ as:

$$\mathcal{F}_m(u) = u\hat{\Phi}_{m,0}(u) + \hat{\varphi}_{m,0}(u) \tag{A1}$$

$$\hat{\Phi}_{m,0}(u) = \frac{1}{2} + \frac{1}{2}\tanh\left(0.7983u + 0.03564u^3\right) \tag{A2}$$

$$\hat{\varphi}_{m,0}(u) = \frac{\mathrm{d}\hat{\Phi}_{m,0}(u)}{\mathrm{d}u} \tag{A3}$$

Then, $\hat{E}_{ep}\left(x \middle| \underline{x}\right)$ can be re-expressed as:

$$\hat{E}_{ep}\left(\sigma_m u + \mu_m \middle| \underline{x}\right) = \sum_{m=1}^{M} \omega_m \sigma_m \mathcal{F}_m(u) - \left(\sigma_m u + \mu_m\right)\hat{\Phi}\left(\underline{x}\right) + \sum_{m=1}^{M} \omega_m\left(\mu_m \hat{\Phi}_m\left(\underline{x}\right) - \sigma_m^2 \varphi_m\left(\underline{x}\right)\right) \tag{A4}$$

If $\mathcal{F}_m(u)$ can be proven convex, (29) is convex.

The second order derivative of $\mathcal{F}_m(u)$ is:

$$\mathcal{F}_m''(u) = 2\hat{\varphi}_{m,0}(u) + u\frac{\mathrm{d}\hat{\varphi}_{m,0}(u)}{\mathrm{d}u} + \frac{\mathrm{d}^2\hat{\varphi}_{m,0}(u)}{\mathrm{d}u^2} \tag{A5}$$

Equation (A5) is an even function and monotonically decreases over interval $[0, +\infty)$. Since the limit of $\mathcal{F}_m''(u)$ is $\lim_{u\to\infty} \mathcal{F}_m''(u) = 0$, $\mathcal{F}_m''(u)$ is positive definite in $\mathbf{R}$. Therefore, (29) is a convex function. The properties of (A5) are described in detail in supplemental file [30].

REFERENCES

[1] F. Liu, X. Wang, F. Sun *et al*., "Correct and remap solar radiation and photovoltaic power in China based on machine learning models," *Applied Energy*, vol. 312, p. 118775, Apr. 2022.

[2] H. Yang, R. Liang, Y. Yuan *et al*., "Distributionally robust optimal dispatch in the power system with high penetration of wind power based on net load fluctuation data," *Applied Energy*, vol. 313, p. 118813, May 2022.

[3] Z. Li, W. Wu, B. Zhang *et al*., "Adjustable robust real-time power dispatch with large-scale wind power integration," *IEEE Transactions on Sustainable Energy*, vol. 6, no. 2, pp. 357-368, Apr. 2015.

[4] L. Moretti, E. Martelli, and G. Manzolini, "An efficient robust optimization model for the unit commitment and dispatch of multi-energy systems and microgrids," *Applied Energy*, vol. 261, p. 113859, Mar. 2020.

[5] X. Zhou, Q. Ai, and M. Yousif, "Two kinds of decentralized robust economic dispatch framework combined distribution network and multi-microgrids," *Applied Energy*, vol. 253, p. 113588, Nov. 2019.

[6] W. -S. Tan and M. Shaaban, "A hybrid stochastic/deterministic unit commitment based on projected disjunctive MILP reformulation," *IEEE Transactions on Power Systems*, vol. 31, no. 6, pp. 5200-5201, Nov. 2016.

[7] Z. Wang, C. Shen, F. Liu *et al*., "Chance-constrained economic dispatch with non-Gaussian correlated wind power uncertainty," *IEEE Transactions on Power Systems*, vol. 32, no. 6, pp. 4880-4893, Nov. 2017.

[8] C. Tang, J. Xu, Y. Sun *et al*., "A versatile mixture distribution and its application in economic dispatch with multiple wind farms," *IEEE Transactions on Sustainable Energy*, vol. 8, no. 4, pp. 1747-1762, Oct. 2017.

[9] R. Lu, T. Ding, B. Qin *et al*., "Multi-stage stochastic programming to joint economic dispatch for energy and reserve with uncertain renew-

able energy," *IEEE Transactions on Sustainable Energy*, vol. 11, no. 3, pp. 1140-1151, Jul. 2020.
[10] S. Wang, H. Gangammanavar, S. D. Eksioglu *et al*., "Stochastic optimization for energy management in power systems with multiple microgrids," *IEEE Transactions on Smart Grid*, vol. 10, no. 1, pp. 1068-1079, Jan. 2019.
[11] K. Bruninx and E. Delarue, "A statistical description of the error on wind power forecasts for probabilistic reserve sizing," *IEEE Transactions on Sustainable Energy*, vol. 5, no. 3, pp. 995-1002, Jul. 2014.
[12] M. Zhang, X. Ai, J. Fang *et al*., "A systematic approach for the joint dispatch of energy and reserve incorporating demand response," *Applied Energy*, vol. 230, pp. 1279-1291, Nov. 2018.
[13] M. Asensio and J. Contreras, "Stochastic unit commitment in isolated systems with renewable penetration under CVaR assessment," *IEEE Transactions on Smart Grid*, vol. 7, no. 3, pp. 1356-1367, May 2016.
[14] N. Zhang, C. Kang, Q. Xia *et al*., "A convex model of risk-based unit commitment for day-ahead market clearing considering wind power uncertainty," *IEEE Transactions on Power Systems*, vol. 30, no. 3, pp. 1582-1592, May 2015.
[15] C. M. Chin and R. Fletcher, "On the global convergence of an SLP-filter algorithm that takes EQP steps," *Mathematical Programming*, vol. 96, no. 1, pp. 161-177, Apr. 2003.
[16] E. Riccietti, S. Bellavia, and S. Sello, "Sequential linear programming and particle swarm optimization for the optimization of energy districts," *Engineering Optimization*, vol. 51, no. 1, pp. 84-100, Jan. 2019.
[17] S. Xu, W. Wu, Y. Yang *et al*., "Analytical solution of stochastic real-time dispatch incorporating wind power uncertainty characterized by Cauchy distribution," *IET Renewable Power Generation*, vol. 15, no. 10, pp. 2286-2301, Jul. 2021.
[18] S. Xu, W. Wu, Y. Sun *et al*., "MIQP reformulation and reliable solution of stochastic economic dispatch," in *Proceedings of 2021 IEEE 5th Conference on Energy Internet and Energy System Integration (EI2)*, Taiyuan, China, Oct. 2021, pp. 256-260.
[19] W. Wei, F. Liu, S. Mei *et al*., "Robust energy and reserve dispatch under variable renewable generation," *IEEE Transactions on Smart Grid*, vol. 6, no. 1, pp. 369-380, Jan. 2015.
[20] Y. Yang, W. Wu, B. Wang *et al*., "Analytical reformulation for stochastic unit commitment considering wind power uncertainty with Gaussian mixture model," *IEEE Transactions on Power Systems*, vol. 35, no. 4, pp. 2769-2782, Jul. 2020.
[21] I. Goodfellow, Y. Bengio, A. Courville *et al*., *Deep Learning*. Cambridge: MIT press, 2016.
[22] J. Shi, Z. Ding, W.-J. Lee *et al*., "Hybrid forecasting model for very-short term wind power forecasting based on grey relational analysis and wind speed distribution features," *IEEE Transactions on Smart Grid*, vol. 5, no. 1, pp. 521-526, Jan. 2014.
[23] N. Ma, Z. Dong, and B. Feng, "Wind power prediction based on signal decomposition and kernel extreme learning machine," *Shandong Electric Power*, vol. 49, no. 1, pp. 1-6, Jan. 2022.
[24] A. A. Mohamed and B. Venkatesh, "Line-wise optimal power flow using successive linear optimization technique," *IEEE Transactions on Power Systems*, vol. 34, no. 3, pp. 2083-2092, May 2019.
[25] S. Xu and W. Wu, "Tractable reformulation of two-side chance-constrained economic dispatch," *IEEE Transactions on Power Systems*, vol. 37, no. 1, pp. 796-799, Jan. 2022.
[26] F. Andersson, H. Mausser, D. Rosen *et al*., "Credit risk optimization with conditional value-at-risk criterion," *Mathematical Programming*, vol. 89, no. 2, pp. 273-291, Jan. 2001.
[27] S. Xu and W. Wu. (2022, Jul.). Test data of the modified IEEE 39-bus system. [Online]. Available: https://drive.google.com/drive/folders/1pgdUzl42qb4RB5jaNxuT92szFA9idvZM
[28] Z.-L. Gaing, "Particle swarm optimization to solving the economic dispatch considering the generator constraints," *IEEE Transactions on Power Systems*, vol. 18, no. 3, pp. 1187-1195, Aug. 2003.
[29] A. M. Fathabad, J. Cheng, K. Pan *et al*., "Asymptotically tight conic approximations for chance-constrained AC optimal power flow," *European Journal of Operational Research*, vol. 305, no. 2, pp. 738-753, Mar. 2023.
[30] S. Xu and W. Wu. (2022, Nov.). Supplemental file of probabilistic energy and reserve co-dispatch for high-renewable power systems and its convex reformulation [Online]. Available: https://www.dropbox.com/s/ziajmychdv9bjrj/SupplementalFile.pdf?dl=0

Shuwei Xu received the B.S. degree in electrical engineering from Shandong University, Jinan, China, in 2018. He is currently working toward the Ph.D. degree with the Department of Electrical Engineering, Tsinghua University, Beijing, China. His research interests include optimization and control in power system.

Wenchuan Wu received the B.S., M.S., and Ph.D. degrees from the Electrical Engineering Department, Tsinghua University, Beijing, China. He is currently a Full Professor with Tsinghua University. He was a recipient of the National Science Fund of China Distinguished Young Scholar Award in 2017. His research interests include energy management system, active distribution system operation and control, machine learning and its application in energy system.

Bin Wang received the B.S. and Ph.D. degrees in electrical engineering from Tsinghua University, Beijing, China, in 2005 and 2011, respectively. He is currently an Associate Professor with the Department of Electrical Engineering, Tsinghua University. His research interests include renewable energy optimal dispatch and control, and automatic voltage control.

Yue Yang received the B.S. and Ph.D. degrees from the Electrical Engineering Department, Tsinghua University, Beijing, China, in 2017 and 2022, respectively. He is currently an Assistant Professor with Hefei University of Technology, Hefei, China. His research interests include optimization and control in power system with integration of renewable energy.